The Journal of Neuroscience, April 1, 1999, *19*(7):2647–2657

Cortical Visuomotor Integration during Eye Pursuit and Eye–Finger Pursuit

Nobuyuki Nishitani,[1] Kimmo Uutela,[1] Hiroshi Shibasaki,[2] and Riitta Hari[1,3]

[1]Brain Research Unit, Low Temperature Laboratory, Helsinki University of Technology, FIN-02015 HUT, Espoo, Finland, [2]Department of Brain Pathophysiology, Kyoto University Graduate School of Medicine, Shogoin, Sakyo-ku, Kyoto, 606–8507, Japan, and [3]Department of Clinical Neurosciences, Helsinki University Central Hospital, FIN-00290, Helsinki, Finland

To elucidate cortical mechanisms of visuomotor integration, we recorded whole-scalp neuromagnetic signals from six normal volunteers while they were viewing a black dot moving linearly at the speed of 4°/sec within a virtual rectangle. The dot changed its direction randomly once every 0.3–2 sec. The subject either (1) fixated a cross in the center of the screen (eye fixation task), (2) followed the moving dot with the eyes (eye pursuit task), or (3) followed the dot with both the eyes and the right index finger (eye–finger pursuit task). Prominent magnetic signals, triggered by the changes of the direction of the dot, were seen in all conditions, but they were clearly enhanced by the tasks and were strongest during the eye–finger pursuit task and over the anterior inferior parietal lobule (aIPL). Source modeling indicated activation of aIPL [Brodmann's area (BA) 40], the posterosuperior parietal lobule (SPL; BA 7), the dorsolateral frontal cortex (DLF; BA 6), and the occipital cortex (BA 18/19). The activation first peaked in the occipital areas, then in the aIPL and DLF, and some 50 msec later in the SPL. Our results suggest that all these areas are involved in visuomotor transformation, with aIPL playing a crucial role in this process.

Key words: visuomotor integration; eye–finger pursuit; smooth pursuit; fixation; MEG; anterior inferior parietal lobule; human

The mammalian visual system is composed of several parallel pathways, each subserving a different aspect of visual experience (Maunsell and Newsome, 1987; Van Essen et al., 1992). Visual processing in the primates can be divided into ventral and dorsal pathways (Ungerleider and Mishkin, 1982). The dorsal stream, projecting from the striate cortex to the parietal region, is concerned with spatial localization of objects of interest, with the composition of motor commands for visually guided actions and with movements related to objects (Goodale and Milner, 1992). It codes spatial characteristics of visual stimuli and mediates visuomotor transformations.

Cortical analysis of visuomotor integration has been extensively made in monkeys. Visuospatial information is preprocessed in visual cortices and then transferred to visual area 5 (V5) and middle temporal area (MT), middle superior temporal area (MST) (Maunsell and Van Essen, 1987; Komatsu and Wurtz, 1988a,b), and parieto-occipital area (PO), and subsequently to several other areas [medial intraparietal area (MIP), ventral intraparietal area (VIP), lateral intraparietal area (LIP), and anterior inferior parietal area (AIP) in the intraparietal sulcus (IPS) and to its proximity (7a and 7b) in the inferior parietal lobule (IPL) (Zeki, 1974; Lynch et al., 1977; Motter and Mountcastle, 1981; Van Essen et al., 1981; Sakata et al., 1983; Felleman and Van Essen, 1991; Colby et al., 1993; Johnson et al., 1996). Neurons of LIP and area 7a discharge in relation to saccades and direction-specific pursuit eye movements (Mountcastle et al., 1975; Lynch et al., 1977, 1985; Sakata et al., 1983; Andersen, 1995; Bremmer et al., 1997; Savaki et al., 1997). Area 7b is related to hand movements (Hyvärinen and Poranen, 1974). Some recent studies showed activity associated with visually guided hand movements in inferior IPS and the adjacent anterior inferior parietal lobule (aIPL) (Gallese et al., 1994; Sakata et al., 1995; Johnson et al., 1996; Savaki et al., 1997).

In addition to the visual pathways in the occipitoparietal areas, the dorsolateral frontal area (DLF) has been shown to be related to oculomotor control and attention to visual stimuli. Both human patients and nonhuman primates with lesions in the DLF show deficits of smooth pursuit eye movements, and microstimulation of this area elicits smooth eye movements (Lynch, 1987; Keating, 1991; MacAvoy et al., 1991; Gottlieb et al., 1993, 1994; Morrow and Sharpe, 1995; Lekwuwa and Barnes, 1996).

Cortical networks of visuomotor transformation have been elucidated in monkeys by the tracing techniques (Andersen et al., 1985, 1990; Ungerleider et al., 1986; Cavada and Goldman-Rakic, 1989a,b; Neal et al., 1990; Jeannerod et al., 1995; Johnson et al., 1996), but they are still insufficiently known in humans despite extensive imaging studies (Grafton et al., 1992; Faillenot et al., 1997; Lacquaniti et al., 1997; Petit et al., 1997; Luna et al., 1998).

In this study, to clarify neural mechanisms underlying human visuomotor integration, we analyzed cortical activation patterns during eye fixation, eye pursuit, and eye–finger pursuit tasks using a whole-scalp magnetoencephalography (MEG), which provides reasonable spatial and excellent temporal resolution.

Received June 5, 1998; revised Jan. 11, 1999; accepted Jan. 17, 1999.

This study was supported by the Academy of Finland, the Sigrid Jusélius Foundation, Japan Foundation for Aging and Health, the Research Grant for the Future Program JSPS-RFTF97L00201 from the Japan Society for the promotion of Science, and Research Grant for International Scientific Research 10044269 from the Japan Ministry of Education, Science, Sports, and Culture. The MRIs were acquired at the Department of Radiology of the Helsinki University Central Hospital. We thank Mr. Mika Seppä for the MRI surface rendering, Dr. Simo Vanni for insightful comments on a previous version of this manuscript, Mr. Ricardo Vigario for support in the additional analyses, and Ms. Mia Illman for assistance in the measurements.

Correspondence should be addressed to Dr. Nobuyuki Nishitani, Brain Research Unit, Low Temperature Laboratory, Helsinki University of Technology, P.O. Box 2200, FIN-02015 HUT, Espoo, Finland.

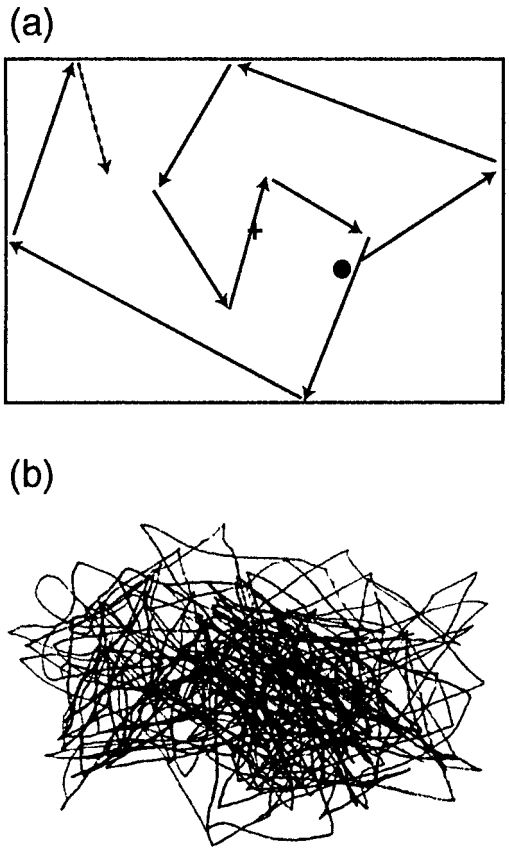

Figure 1. *a*, Schematic illustration of the visual stimulus. A *black dot* (radius, 0.57°) moved linearly within a virtual rectangle of 30 × 40 cm at the speed of 4°/sec and changed randomly its direction once every 0.3–2 sec. *b*, The subject's finger movements during the eye–finger pursuit task, traced with a small pen fixed to the right index finger.

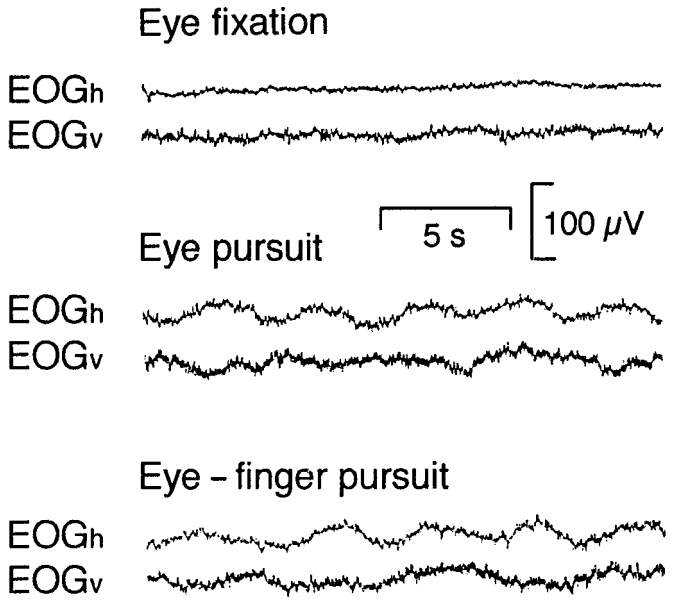

Figure 2. Horizontal and vertical electro-oculograms (*EOGh* and *EOGv*) during the eye fixation, eye pursuit, and eye–finger pursuit tasks from subject 1.

MATERIALS AND METHODS

Subjects

Six healthy volunteers (four males and two females, age 25–40 years, mean 30; five right-handed and one left-handed) were studied. None of them had previous history of neurological or visual disorders. Informed consent was obtained from each subject after full explanation of the study.

Experimental paradigm

During the experiment, the subject was sitting in a magnetically shielded room. The head was positioned in a helmet-shaped dewar and closely attached against its inner vault. The visual stimuli, produced with MacProbe running on a Macintosh Quadra 840 AV computer, were projected onto a white board placed 1 m in front of the subject, with a Sony data projector that was positioned outside the magnetically shielded room. The subject was viewing the screen in dim light. A black dot (radius, 0.57°) was moved linearly within a virtual rectangle of 30 × 40 cm at the speed of 4°/sec, and it changed randomly its direction once every 0.3–2 sec (Fig. 1*a*). The recording time for each block was 3 min on the average. The subject was asked either (1) to fixate a cross on the center of the screen (eye fixation task), (2) to follow the moving dot with the eyes (eye pursuit task), or (3) to follow it with both the eyes and the right index finger (eye–finger pursuit task). During the latter task, the subject kept the right index finger on her/his lap and was asked to draw on a paper the lines precisely mimicking the trajectory of the visual target with a small pen attached to the finger tip (Fig. 1*b*).

Data acquisition

The magnetic signals of the brain were measured with a helmet-shaped 122-channel Neuromag-122 neuromagnetometer, which uses 61 pairs of orthogonally arranged "figure eight" planar first-order gradiometers. This system measures the two orthogonal derivatives of the radial magnetic field component (Ahonen et al., 1993), and it typically detects the largest signal just above the corresponding cerebral current source. Head position with respect to the sensor array was measured with head position indicator (HPI) coils placed on defined scalp sites. To allow alignment of the MEG and magnetic resonance imaging (MRI) coordinate systems, the positions of the HPI coils with respect to anatomical landmarks were measured with a three-dimensional digitizer (Isotrak 3S1002; Polhemus Navigation Sciences, Colchester, VT). At the beginning of each recording block, the magnetic signals produced by the three HPI coils on the scalp were measured by the sensors to obtain head position with respect to the sensor array. Head position was recalculated at the start of each block. Head MRIs were obtained with a 1.5 tesla Siemens Magnetom system. To monitor eye movements and blinks, bipolar horizontal and vertical electro-oculograms (EOGh and EOGv, respectively) were recorded from electrodes placed below and above the left eye and to bilateral outer canthi. To monitor the subject's vigilance, the waveforms of EOG and selected channels of MEG were inspected continuously during the recording. The subject could refresh during short breaks between the blocks, but he or she was requested to maintain the head position as stable as possible during the intermissions. The recording bandpass was 0.03–100 Hz (3 dB points) for MEG and 0.01–100 Hz (6 dB points) for EOG. The sampling rate for digital conversion was 404 Hz, and the data were stored on an optical disk for later off-line analysis. In the beginning of the task, the background brain activity was recorded for 3 min while the subject was fixating a cross placed on the center of the screen. To confirm the signal reproducibility, the data were collected during two to four identical blocks for each task, and the order of tasks was counterbalanced across subjects. Blocks contaminated with excessive artifacts (eye movements, blinks, noise) in any of the channels, or with drowsiness of the subject, were excluded from the analysis, and an additional block was acquired.

Data analysis

Signal analysis. We analyzed only those signals associated with stimulus triggers separated by at least 1 sec from the preceding and following ones. The signals were averaged off-line from 100 msec before to 900 msec after the time when the visual target changed its direction, separately for the three different conditions. Epochs containing MEG signals exceeding 1500 fT/cm and/or EOG signals exceeding 150 μV were omitted. Amplitudes were measured with respect to the 100 msec pretrigger baseline for each channel.

Source modeling. After confirming the individual reproducibility of the

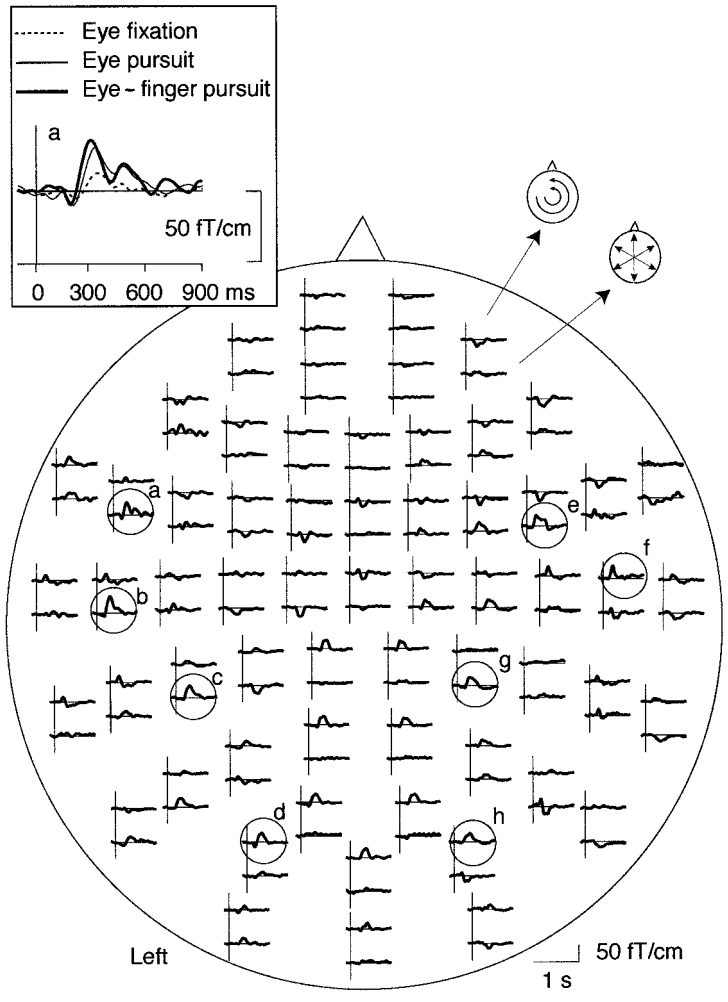

Figure 3. Whole-scalp magnetic responses of subject 1 during the eye–finger pursuit task. The head is viewed from above, and the *top* and *bottom* traces of each response pair show the latitudinal and longitudinal derivatives of the magnetic field perpendicular to the helmet at the measurement site. Responses from the left frontal area are magnified in the *left top corner*, superimposed with the responses obtained during other two tasks. *Encircled* locations refer to the channels that are illustrated for all subjects in Figure 4.

MEG waveforms, the data of two blocks per task were averaged, and the averages were digitally low-pass filtered at 40 Hz. The preprocessed data were used for construction of isocontour maps. The sources of the magnetic fields were modeled as equivalent current dipoles (ECDs) whose three-dimensional locations, orientations and current strengths were estimated from the preprocessed data using a least-squares method. A spherical head model was adopted, based on the individual MRI obtained from each subject (Hämäläinen et al., 1993).

The ECDs that best explained the most dominant signals were determined from signals of 20–30 channels at areas including the local signal maxima. For each subset of channels, ECDs were calculated for every 1msec segment over the time period of 50 msec containing the signal maximum. We only accepted ECDs that could account for >80% of the field variance at selected periods of time for each subset of channels and whose confidence volume (Hämäläinen et al., 1993) was <1 cm^3. ECDs with the highest percentage of explained variance and the smallest confidence volume were accepted for further analysis. Thereafter, the analysis period was extended to the whole recording time and to all channels, using a multidipole model in which the strengths of the previously found ECDs were allowed to vary as a function of time while their locations and orientations were kept fixed (Scherg and Von Cramon, 1986; Mosher et al., 1992; Scherg, 1992; Hämäläinen et al., 1993). Such multiple dipoles are assumed to model satisfactorily the combined activity arising from several brain regions when the activation spots, each <2–4 cm in diameter, overlap in time but are spatially distinct.

The measured signals explained by the model were extracted with Signal Space Projection (Uusitalo and Ilmoniemi, 1997), and a new ECD was identified on the basis of the remaining field pattern. Every time when a new ECD was obtained, the waveforms predicted by the multidipole model were compared with the measured signals. If the model left some dominant signals unexplained, the data were re-evaluated for more accurate estimation of the generator areas, but with a conservative attitude to explain only the dominant features of the field pattern. This approach, described in detail previously (Hämäläinen et al., 1993), has been successfully applied in several previous reports (Hari et al., 1993; Forss et al., 1994; Levänen et al., 1996; Raij et al., 1997; Nishitani et al., 1998).

Finally, the estimated dipoles obtained through this procedure were superimposed on the subject's own MRI, after alignment of the MEG and MRI coordinate systems. For the transformation of the source locations to the Talairach's standard brain space (Talairach and Tournoux, 1988), the following coordinate system was used: *x*-axis perpendicular to the other two axes through the anterior commissure, *y*-axis passing through the anterior and posterior commissure, and *z*-axis perpendicular to the *y*-axis through the anterior commissure at the middle plane of the brain. The source locations were transformed into the standard brain space with spatial normalization by matching each subject's brain to a standard brain space. The coordinates *x* (left/right), *y* (anterior/posterior), and *z* (superior/inferior) were expressed in millimeters from the anterior commissure at the midline of the brain. Brodmann's areas (BA) were defined according to the atlas of Talairach's standard brain space.

Furthermore, the validity of the multidipole model was confirmed by using L1 Minimum Norm Estimate (L1 MNE), which can resolve several local or distributed MEG current sources without explicit *a priori* information about the number of sources (Uutela et al., 1997). The L1 MNE is the current distribution where the total sum of the current is as small as possible, while it still explains almost all the measured signals. The estimated source distributions were visualized by projecting the currents to the surface of the subject's brain.

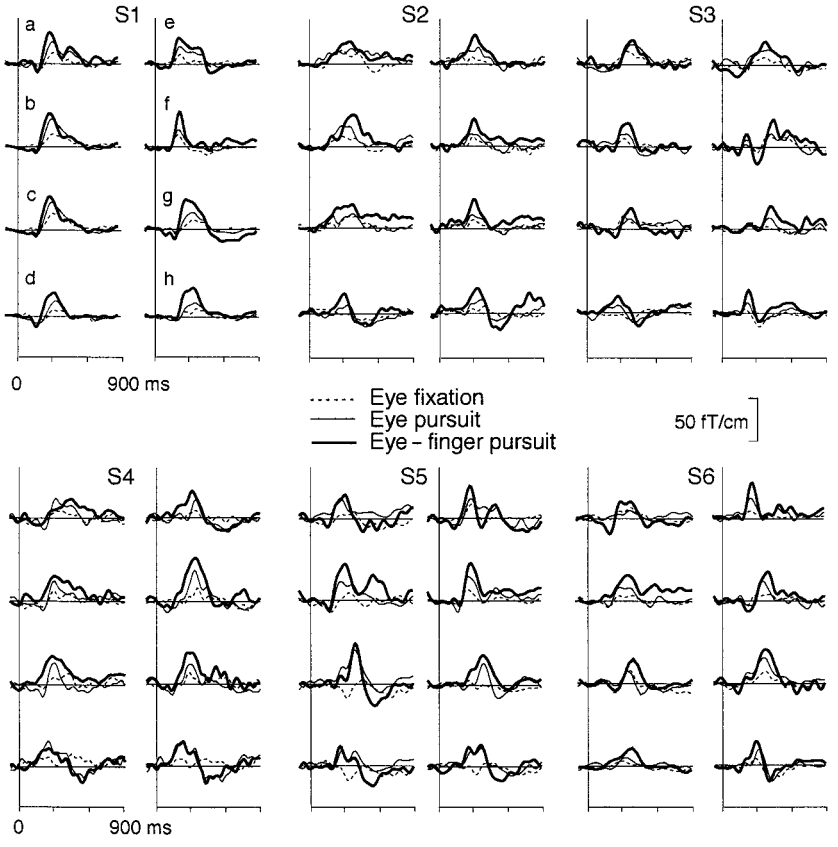

Figure 4. Magnetic responses of all subjects over the anterior (*a*, *e*), middle (*b*, *c*, *f*, *g*), and posterior (*d*, *h*) channels on each hemisphere during the eye fixation (*dotted lines*), eye pursuit (*thin lines*), and eye–finger pursuit tasks (*thick lines*). For measurement locations, see Figure 3.

Statistical analysis

The latencies and strengths of the sources were compared with an ANOVA with repeated measurements. The factors analyzed were task, measurement location, and response laterality. The peak latencies were scaled relative to the peak latency of the aIPL source (see below) in each subject.

RESULTS

Waveforms

In the fixation task, both EOGv and EOGh were stable in all subjects. In the eye pursuit and eye–finger pursuit tasks, both EOGs showed oscillations, reflecting pursuit eye movements (Fig. 2).

Figure 3 shows typical MEG signals from subject 1. The largest magnetic deflections peaked 200–400 msec after the time when the visual target changed its direction. Prominent responses were observed at wide areas bilaterally during all tasks.

Figure 4 illustrates that all subjects had clear magnetic deflections time-locked to changes of the direction of the dot. The main deflections peaked at 200–450 msec in different subjects and were consistently largest during the eye–finger pursuit task.

Source modeling

At the main response peaks, the magnetic field patterns were dipolar over several regions of both hemispheres, although with clear interindividual variability. Figure 5 shows field patterns of subject 4 over the right hemisphere. These patterns suggested four main source areas (occipital cortex, IPL, DLF, and SPL), which were similar across tasks except for the IPL region in the eye fixation task in which no clear ECD was identified. Similar dipolar patterns were seen on this subject's left hemisphere for all tasks and also in other subjects. Similarly to subject 4, no dipolar patterns were seen during the eye fixation task on the left hemisphere in three subjects and on the right hemisphere in two subjects.

Figure 6 shows the sources of magnetic fields from subject 4 superimposed on his own MRI. During the eye fixation task, the main sources were located in DLF, aIPL, and SPL of each hemisphere. In the eye pursuit and eye–finger pursuit tasks, additional sources were observed in the occipital cortex of each hemisphere. Despite interindividual variability in the field patterns and the number of dipoles, there was a considerable consistency in the source locations across subjects and tasks (Fig. 7). Table 1 summarizes the source locations in Talairach coordinates in each area and for all tasks; the source locations did not differ significantly between hemispheres in any task ($p > 0.87$).

Figure 8 shows an independent evaluation of the activation pattern of the brain with L1 MNEs during the eye–finger pursuit task for subject 4. Compared with the data presented in Figures 5 and 6, the current estimates were in good agreement with the dipole models, implying the activation in the occipital cortex, aIPL, DLF, and SPL of each hemisphere.

Figure 9 shows the strengths of all eight dipoles (four sources in each hemisphere) calculated from a multidipole model during the eye–finger pursuit task for subject 1. The activations peaked at 220 and 265 msec in the left and right occipital areas, at 278 and 330 msec in the left and right aIPL, at 292 and 284 msec in the left and right DLF, and at 350 and 374 msec in the left and right SPL, each respectively. The 8-dipole model explained the signal distributions best ($g > 90\%$) at 280–325 msec.

Figure 10 (*top*) shows the mean (+ SEM) source strengths in the four brain regions during all tasks. The sources were of about the same strength in all areas during the eye fixation task. During

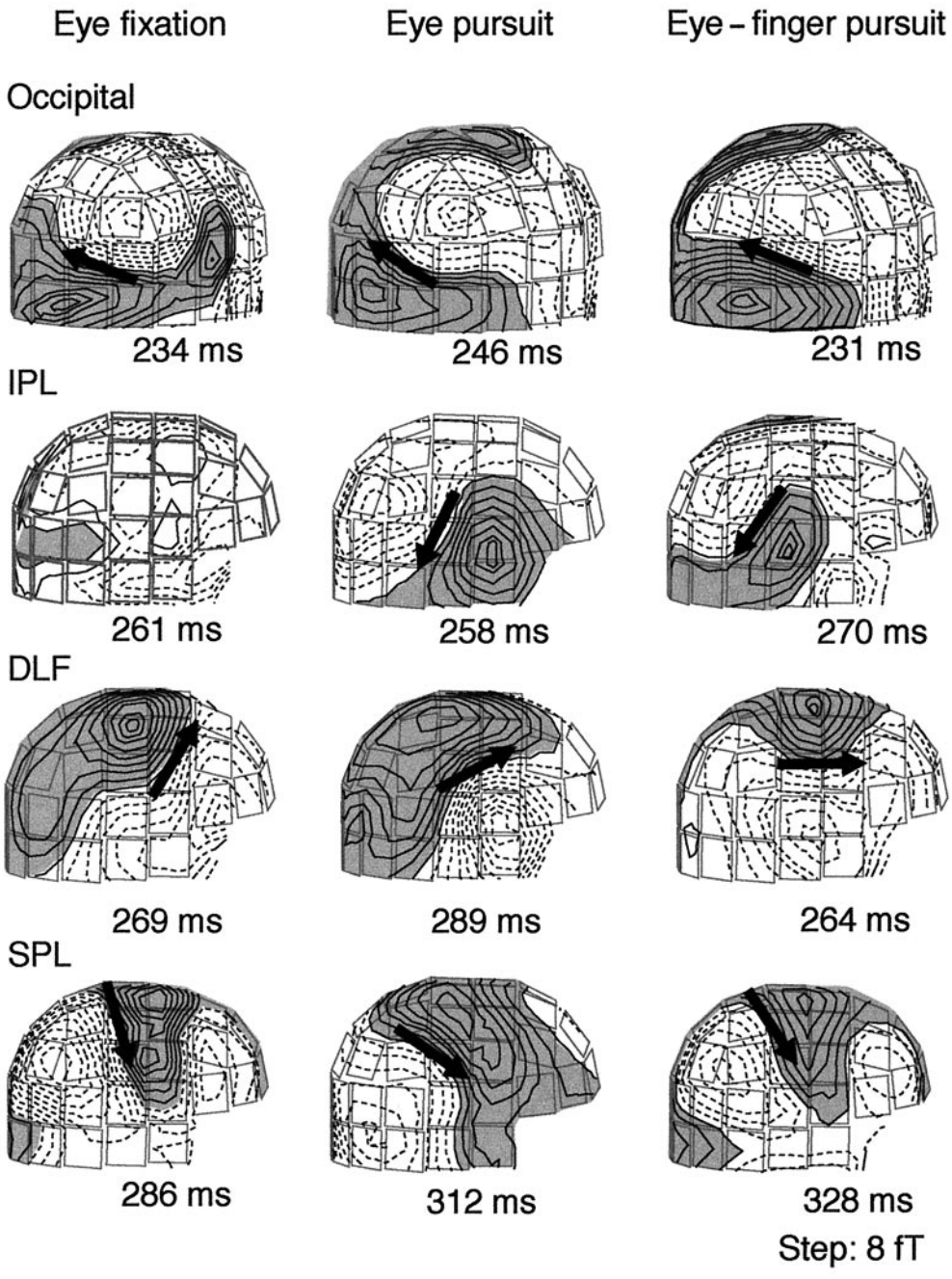

Figure 5. Magnetic field patterns of subject 4 during the eye fixation (*left*), eye pursuit (*middle*), and eye–finger pursuit tasks (*right*). The magnetic isocontour lines are separated by 8 fT. *Shaded areas* with *solid lines* illustrate the magnetic flux emerging from the head, and the areas with *dotted lines* illustrate the flux into the head. *Arrows* illustrate the locations and directions of the ECDs for dipolar field patterns; note that no ECD fulfilling the criteria was found in the IPL region during the eye fixation task.

the eye pursuit and eye–finger pursuit tasks, no modification was seen in the occipital area, whereas in the other regions the sources were significantly stronger; the most prominent activation occurred during the eye–finger pursuit task in the aIPL; the signals were significantly stronger during the eye pursuit and eye–finger pursuit than the eye fixation task ($p < 0.005$). A similar trend did not reach statistical significance in the other regions. There was a statistically nonsignificant trend for stronger right than left hemisphere sources (mean differences 13% during eye fixation, 18% during eye pursuit, and 5% during eye–finger pursuit).

Figure 10 (*bottom*) shows the peak latencies of activation in DLF, SPL, and occipital areas relative to latencies in the aIPL. Earliest activation occurred in the occipital areas ($p < 0.05$) followed by the signals in the aIPL. Activation tended to peak slightly later in the DLF than the aIPL (NS), and the activation peaked on average 55 msec later in the SPL than the aIPL ($p < 0.005$). The mean latencies did not differ significantly between the hemispheres in any of these areas.

DISCUSSION

Activated brain areas and their temporal order

This study aimed to clarify human cortical mechanisms of visuomotor integration. Strong magnetic signals were triggered by changes of the direction of the dot in four main brain areas: the occipital cortex and areas aIPL, DLF, and SPL, which, according to the Talairach coordinates, correspond anatomically to Brodmann's areas 18/19, 40, 6, and 7, respectively.

The aIPL showed the strongest signals in all conditions. The

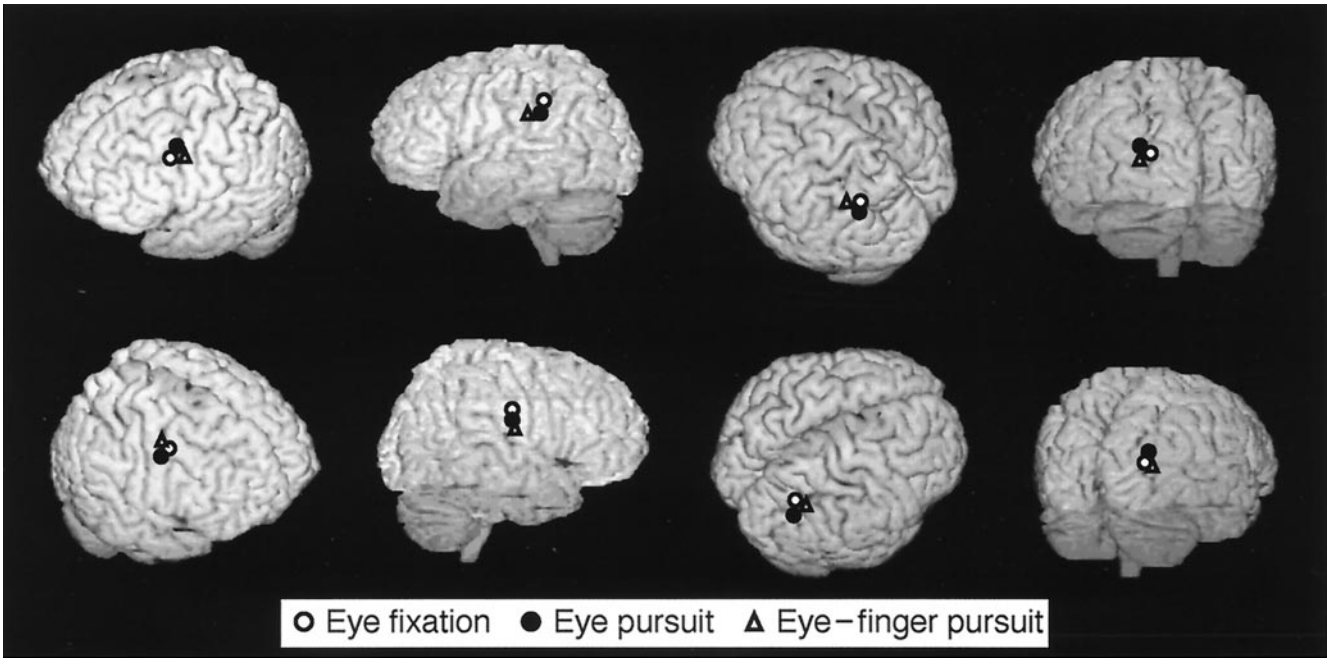

Figure 6. The main source locations for subject 4 in the eye fixation, eye pursuit, and eye–finger pursuit tasks, superimposed on the subject's own three-dimensional MRI. *Top* and *bottom* figures show the surface of brain viewed from *left* and *right* sides, respectively.

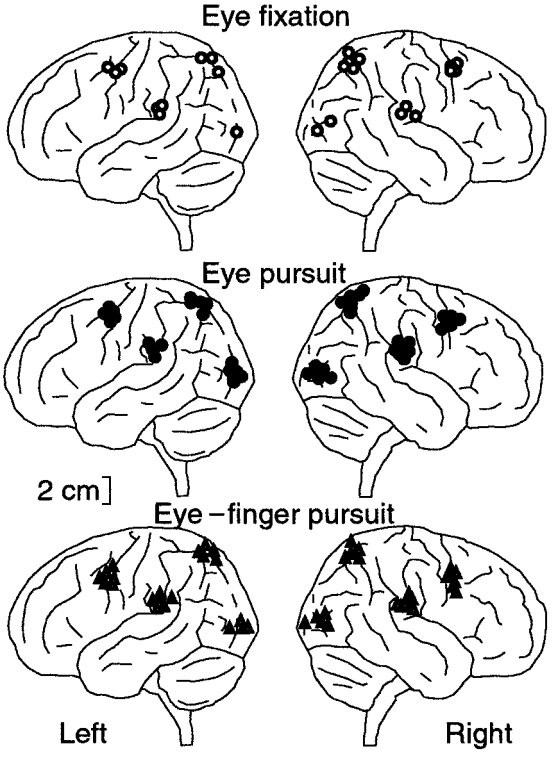

Figure 7. ECD locations for the eye fixation, eye pursuit, and eye–finger pursuit tasks from all subjects projected on a schematic brain viewed from *left* and *right* sides. The locations were normalized onto a schematic brain according to Talairach's human atlas (Talairach and Tournoux, 1988).

pursuit tasks increased the activity of all areas but most strongly that of aIPL, in which the source strength was almost tripled during the eye–finger pursuit task compared with the eye fixation task. Our aIPL region was located within 15 mm from the positron emission tomography (PET) activations observed during visually guided grasping task, but ~30 mm dorsolateral to the PET activations during reaching task, and ~25 mm anterolateral and inferior to the functional magnetic resonance imaging (fMRI) spots observed during visually guided saccades (Faillenot et al., 1997; Lacquaniti et al., 1997; Luna et al., 1998).

The present results suggest that the aIPL plays a crucial role in the visuomotor integration during the pursuit tasks. This proposal is supported by clinical observations. The right aIPL is involved in visuospatial attention (Mesulam, 1981), and its lesions cause visual neglect (Heilman et al., 1985; Vallar and Perani, 1986; Rizzolatti and Gallese, 1998). The slowness and prolonged accelerations of contralesional movements in patients with visual neglect, but with intact primary motor area, suggest that the human aIPL not only plays a role in the visuomotor planning but also operates as a sensorimotor interface, rather than having exclusively perceptual or motor functions (Mattingley et al., 1994, 1998; Andersen et al., 1997; Snyder et al., 1997).

Patients with lesions centered on the inferior IPS and SPL may have "optic ataxia" in which they cannot use visual information for accurate control of visually guided hand movements or to accurately reach targets (Perenin and Vighetto, 1988; Grafton et al., 1992; Jackson and Husain, 1997). The observed activation of the SPL may be related to visuospatial attention required to follow the moving dot in the pursuit task (Posner et al., 1984; Corbetta, 1998). The activated SPL region is 7–15 mm lateral to the fMRI activations related to attention to visual motion and 10 mm superior to the mean PET activations during the visuospatial attention task (Nobre et al., 1997; Buchel et al., 1998). The attentional processing in this region of the SPL may also be tightly linked to oculomotor processes, and SPL is likely to play a critical role in movement selection (Deiber et al., 1991).

It is generally believed that sensorimotor coordination involves parallel modules (Stein, 1992; Savaki et al., 1997). Our data also provide an evidence on sequential processing in human visuomo-

Table 1. Source locations in Talairach coordinates (mean ± SEM)

	Left hemisphere			Right hemisphere		
	x	*y*	*z*	*x*	*y*	*z*
Eye fixation						
DLF	−41.4 ± 5.2	−5.0 ± 8.6	40.7 ± 6.2	45.0 ± 9.3	−1.1 ± 4.7	41.9 ± 4.0
aIPL	−61.3 ± 5.0	−33.0 ± 5.1	28.2 ± 4.8	60.6 ± 6.5	−36.7 ± 5.2	24.1 ± 3.0
SPL	−39.6 ± 10	−53.3 ± 6.2	49.9 ± 4.2	36.6 ± 10	−56.6 ± 3.5	50.1 ± 6.2
Occipital	−26.1	−74.7	6.2	31.5 ± 12	−73.4 ± 8.4	3.96 ± 4.9
Eye pursuit						
DLF	−37.5 ± 6.1	−5.5 ± 6.2	45.8 ± 4.4	44.4 ± 6.2	−1.2 ± 7.1	39.0 ± 4.2
aIPL	−59.4 ± 6.5	−32.8 ± 4.7	26.0 ± 4.3	59.1 ± 6.4	−38.5 ± 6.1	26.7 ± 6.6
SPL	−37.8 ± 5.2	−56.0 ± 11	50.5 ± 3.6	36.6 ± 8.6	−56.9 ± 7.2	51.3 ± 5.8
Occipital	−27.3 ± 6.3	−78.2 ± 7.2	8.17 ± 5.2	32.2 ± 3.8	−80.5 ± 10	5.76 ± 5.2
Eye-finger pursuit						
DLF	−41.2 ± 5.0	−2.1 ± 5.6	39.2 ± 6.1	46.0 ± 5.6	−0.9 ± 3.2	40.4 ± 7.0
aIPL	−58.7 ± 3.1	−32.5 ± 4.9	26.7 ± 4.7	59.7 ± 6.0	−35.1 ± 5.8	26.0 ± 4.4
SPL	−37.4 ± 8.9	−55.1 ± 9.1	45.5 ± 8.1	41.4 ± 8.6	−52.8 ± 4.2	48.7 ± 3.4
Occipital	−34.5 ± 8.9	−76.0 ± 8.1	11.0 ± 3.9	33.8 ± 10	−83.3 ± 5.7	11.9 ± 2.0

Coordinates *x* (postive to right), *y* (postive to anterior), *z* (postive upward) are in millimeters from the point of origin situated at the anterior commissure.

tor integration. The activation peak was ~50 msec earlier in the aIPL than in the SPL during both pursuit tasks. Thus, the SPL might obtain input either from the aIPL or the DLF, in addition to the occipital area, which is in agreement with the view that the parietal lobe is the final stage of the dorsal visual stream (Ungerleider and Mishkin, 1982).

Monkey homologs of human IPL and SPL areas

Hyvärinen (1981) suggested that the most anterior part of the human IPL, activated in the present study, corresponds to the monkey 7b, which is related to hand manipulation and eye movements and may code orientation of different body parts in the immediate extrapersonal space (Hyvärinen and Poranen, 1974; Mountcastle et al., 1975; Hyvärinen, 1981). Our data agree with a recent PET study showing that a visually guided pursuit task activates the dorsolateral visual pathways that are connected with the aIPL (Faillenot et al., 1997). The strongest MEG signals in the eye–finger pursuit task in the aIPL thus agree with the properties of monkey 7b. Also in line with monkey data (Hyvärinen, 1981; Andersen et al., 1990), we observed bilateral activation

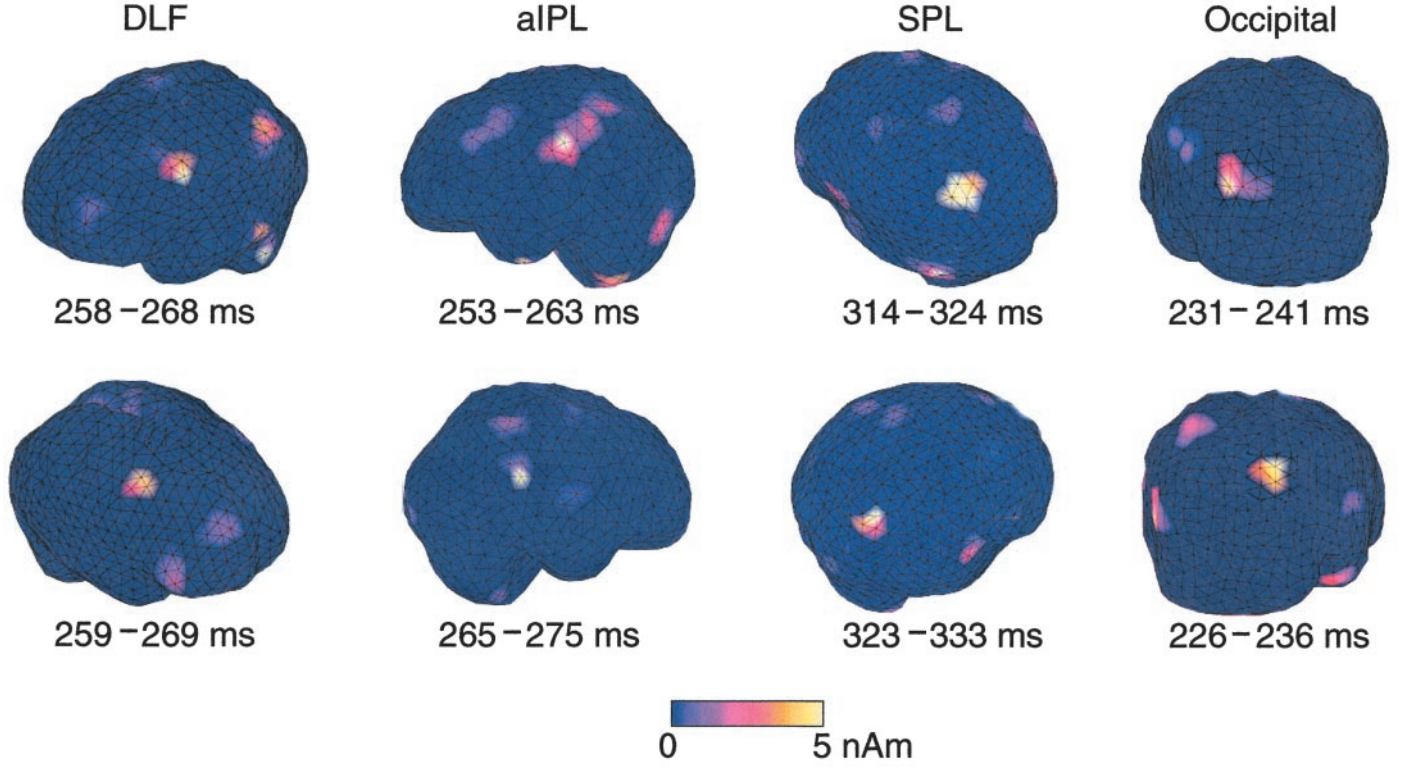

Figure 8. L1 MNEs of currents in both hemispheres during the eye–finger pursuit task in subject 4. Strengths of the current estimates are shown as the averages of the current amplitudes during a 10 msec segment centered on the signal peaks indicated in Figure 5.

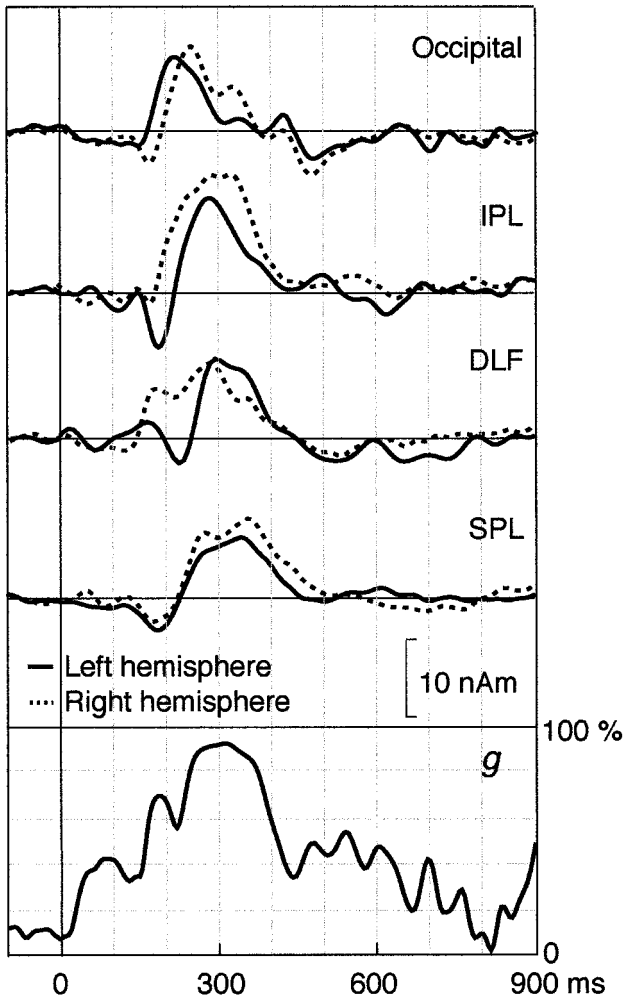

Figure 9. Strengths of all dipoles as a function of time by the time-varying 8-dipole model explaining the data of subject 1 during the eye–finger pursuit task. The *lowest trace* shows the goodness-of-fit of the model.

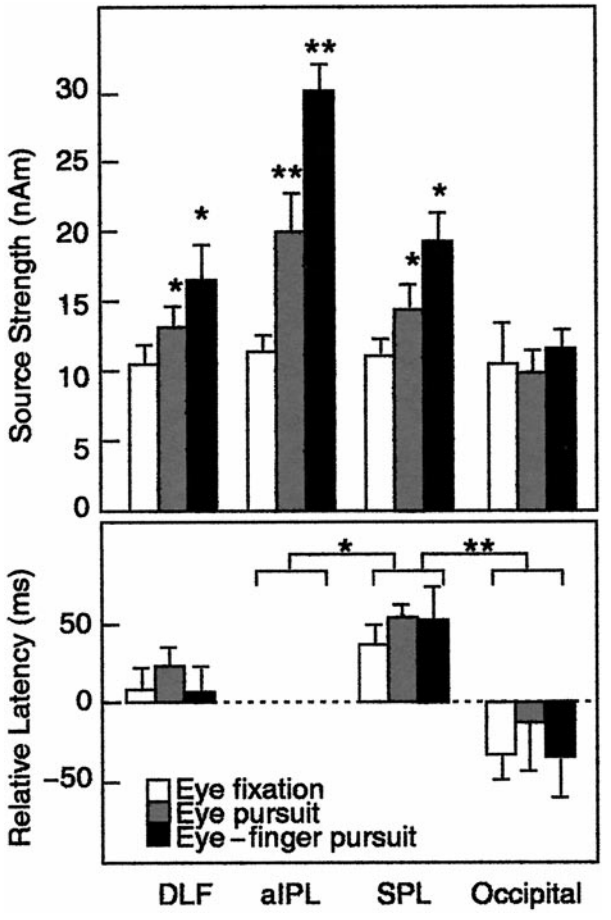

Figure 10. *Top*, Mean (+ SEM) source strengths in all four areas and three conditions; averages of left and right hemisphere data. $^{*}p < 0.05$; $^{**}p < 0.005$ as compared with the eye fixation. *Bottom,* Mean (+ SEM) peak latencies of source waveforms in all four areas, scaled according to individual latencies in the aIPL (absolute values are indicated). $^{*}p < 0.05$; $^{**}p < 0.005$ as compared with aIPL.

of aIPL during the right index finger pursuit task. Thus, our results are in line with the assumption that the human aIPL is the homolog of the monkey area 7b (Hyvärinen, 1981; Eidelberg and Galaburda, 1984). The monkey 7b is connected reciprocally to SII, AIP, and 7a and to the ventral premotor cortex, and it is a part of the network for producing motor responses to visual and somatosensory stimuli (Andersen et al., 1990; Neal et al., 1990; Graziano et al., 1994).

The monkey area 7a responds more strongly to attended than nonattended stimuli (Mountcastle et al., 1981; Steinmetz and Constantinidis, 1995) and is related to direction-specific eye movements (Mountcastle et al., 1975; Lynch et al., 1977, 1985; Sakata et al., 1983; Andersen, 1995; Bremmer et al., 1997; Savaki et al., 1997). The human posterior eye fields are located in precuneus and along the IPS extending into the superior IPL and SPL (Muri et al., 1996; Luna et al., 1998), and they are related to triggering of reflexive visually guided saccades (Pierrot-Deseilligny, 1994; Pierrot-Deseilligny et al., 1995). Our results would thus be in line with the human SPL being the homolog of the monkey 7a.

The significant strengthening of aIPL and SPL activations during both pursuit tasks agrees with monkey data showing that many visual neurons in areas 7a and 7b respond better to moving than stationary stimuli (Motter and Mountcastle, 1981). It is to be noted, however, that the parcellation of the human parietal cortex to functionally homogeneous areas is still largely unknown.

Activation of the dorsolateral frontal cortex

We observed activation of DLF (BA 6) in all tasks, presumably caused by the smooth eye pursuit movements and the visuospatial attention aroused by the changes of the direction of the dot. The human frontal eye field (FEF) is located in BA 6 at the junction of the precentral and the superior frontal sulci (Kleinschmit et al., 1994; Darby et al., 1996; Muri et al., 1996; Paus, 1996; Sweeney et al., 1997; Luna et al., 1998). Our DLF area was ~10 mm anterior to the PET activations observed when subjects followed a visual dot target moving horizontally (Petit et al., 1997). This may suggest the existence of FEF subregions for the oculomotor control related to movement direction. Lesions in the precentral sulcus between the superior and inferior frontal sulci and in the adjacent parts of the precentral gyrus and of the middle frontal gyrus, in good agreement with our source locations, produce deficits of smooth pursuit eye movements (Rivaud et al., 1994; Morrow and Sharpe, 1995; Lekwuwa and Barnes, 1996).

The areas around the arcuate sulcus in monkey may thus be homologous to the posterior bank of the human precentral sulcus

(BA 6). The importance of this region for eye movements is evident from studies in nonhuman primates: ablation of the anterior bank of the arcuate gyrus degrades smooth pursuit eye movements (Lynch, 1987; Keating, 1991; MacAvoy et al., 1991), and microstimulation of this region elicits smooth eye movements (MacAvoy et al., 1991; Gottlieb et al., 1993, 1994). Tanaka and Fukushima (1998), recording electric responses related to smooth pursuit eye movements from the periarcuate area, suggested that the periarcuate neurons participate in the early stages of pursuit initiation.

Absence of phasic activation in parieto-occipital sulcus, V5, and motor cortex

Some recent MEG data have revealed that the human medial parieto-occipital sulcus (POS) area may be the human homolog of the monkey visual area 6 (V6) and visual area 6A (V6A) complex, which is well equipped for encoding visuospatial information related to visually guided movements (Galletti et al., 1995, 1997; Hari et al., 1994; Jousmäki et al., 1996; Hari and Salmelin, 1997). The absence of phasic activation of the medial POS with the present continuous visual motion suggests that the POS region is most reactive to onsets and offsets of the stimuli. In a similar manner, the lack of clear V5 activation, time-locked to changes of the dot movement, indicates that a change in the direction of the dot per se does not produce a sufficiently strong phasic change in V5 activation, at least when responses to changes of all directions are averaged. Furthermore, although the motor cortex is definitely active during voluntary finger movements, there were no detectable signals associated with the changes of movement direction; neither were any systematic changes detected in the rhythmic activity of the motor cortex (our unpublished observations). It has to be emphasized that the signals of the POS region, the V5 cortex, and the primary motor cortex are quite easy to be discriminated by means of whole-scalp MEG recordings (Salenius et al., 1997; Vanni et al., 1997; Portin et al., 1998), and thus we feel confident to claim that these areas did not show major phasic activity associated with changes of the direction of the dot.

Conclusions

Despite the restrictions caused by the nonuniqueness of the neuromagnetic inverse problem (Hämäläinen et al., 1993), we found largely consistent activation of multiple source areas, confirmed by an independent analysis based on minimum-norm current estimates. Our data demonstrate that the occipital cortex, the aIPL, DPL, and SPL areas are all involved in visuomotor integration. The anterior inferior parietal lobules of both hemispheres were activated ~50 msec earlier than the SPL, whereas the DLF was activated at about the same time as the aIPL. Compared with fMRI and PET data, which reflect blood flow changes related to brain activation, the MEG signals directly reflect neuronal activation, mainly postsynaptic currents, and can thus provide complementary information to other human imaging studies. Our data support the view that the aIPL might be the homolog of the monkey area 7b and that it probably plays a pivotal role in the visuomotor integration.

REFERENCES

Ahonen AI, Hämäläinen MS, Kajola MJ, Knuutila JET, Laine PP, Lounasmaa OV, Parkkonen LT, Simola JT, Tesche CD (1993) 122-channel SQUID instrument for investigating the magnetic signals from the human brain. Physica Scripta T49:198–205.

Andersen RA (1995) Encoding of intention and spatial location in the posterior parietal cortex. Cereb Cortex 5:457–469.

Andersen RA, Asanuma C, Cowan WM (1985) Callosal and prefrontal association projecting cell populations in area 7A of the macaque monkey: a study using retrogradely transported fluorescent dyes. J Comp Neurol 232:443–455.

Andersen RA, Asanuma C, Essick G, Siegel RM (1990) Cortico-cortical connections of anatomically and physiologically defined subdivisions within the inferior parietal lobule. J Comp Neurol 296:65–113.

Andersen RA, Lawrence HS, David CB, Jing X (1997) Multimodal representation of space in the posterior parietal cortex and its use in planning movements. Annu Rev Neurosci 20:303–330.

Bremmer F, Distler C, Hoffmann KP (1997) Eye position effects in monkey cortex. pursuit- and fixation-related activity in posterior parietal area LIP and 7A. J Neurophysiol 77:962–977.

Buchel C, Josephs O, Rees G, Turner R, Frith CD, Friston KJ (1998) The functional anatomy of attention to visual motion. A functional MRI study. Brain 121:1281–1294.

Cavada C, Goldman-Rakic PS (1989a) Posterior parietal cortex in rhesus monkey: I. Parcellation of areas based on distinctive limbic and sensory corticocortical connections. J Comp Neurol 287:393–421.

Cavada C, Goldman-Rakic PS (1989b) Posterior parietal cortex in rhesus monkey: II. Evidence for segregated corticocortical networks linking sensory and limbic areas with the frontal lobe. J Comp Neurol 287:422–445.

Colby CL, Duhamel JR, Goldberg ME (1993) Ventral intraparietal area of the macaque: anatomic location and visual response properties. J Neurophysiol 69:902–914.

Corbetta M (1998) Frontoparietal cortical networks for directing attention and the eye to visual locations: identical, independent, or overlapping neural systems? Proc Natl Acad Sci USA 95:831–838.

Darby DG, Nobre AC, Thangaraj V, Edelman R, Mesulam MM, Warach R (1996) Cortical activation in the human brain during lateral saccades using EPISTAR functional magnetic resonance imaging. NeuroImage 3:53–62.

Deiber MP, Passingham PE, Colebatch JG, Friston KJ, Nixon PD, Frackowiak RSJ (1991) Cortical areas and the selection of movement: a study with positron emission tomography. Exp Brain Res 84:393–402.

Eidelberg D, Galaburda AM (1984) Inferior parietal lobule. Divergent architectonic asymmetries in the human brain. Arch Neurol 41:843–852.

Faillenot I, Toni I, Decety J, Gregoire MC, Jeannerod M (1997) Visual pathways for object-oriented action and object recognition: functional anatomy with PET. Cereb Cortex 7:77–85.

Felleman DJ, Van Essen DC (1991) Distributed hierarchical processing in the primate cerebral cortex. Cereb Cortex 1:1–47.

Forss N, Hari R, Salmelin R, Ahonen A, Hämäläinen M, Kajola M, Knnutila J, Simola J (1994) Activation of the human posterior parietal cortex by median nerve stimulation. Exp Brain Res 99:309–315.

Gallese V, Murata A, Kaseda M, Niki N, Sakata H (1994) Deficit of hand preshaping after muscimol injection in monkey parietal cortex. NeuroReport 5:1525–1529.

Galletti C, Battaglini PP, Fattori P (1995) Eye position influence on the parieto-occipital area PO (V6) of the macaque monkey. Eur J Neurosci 7:2486–2501.

Galletti C, Fattori P, Kutz DF, Battaglini PP (1997) Arm movement-related neurons in the visual area V6A of the macaque superior parietal lobule. Eur J Neurosci 9:410–413.

Goodale MA, Milner AD (1992) Separate visual pathways for perception and action. Trends Neurosci 15:20–25.

Gottlieb JP, Bruce CJ, MacAvoy MG (1993) Smooth eye movement elicited by microstimulation in the primate frontal eye field. J Neurophysiol 69:786–799.

Gottlieb JP, MacAvoy MG, Bruce CJ (1994) Neural responses related to smooth-pursuit eye movements and their correspondence with electrically elicited smooth eye movements in the primate frontal eye field. J Neurophysiol 72:1634–1653.

Grafton ST, Mazziotta JC, Woods RP, Phelps ME (1992) Human functional anatomy of visually guided finger movements. Brain 115:565–587.

Graziano SA, Yap GS, Gross CG (1994) Coding of visual space by premotor neurons. Science 266:1054–1056.

Hämäläinen M, Hari R, Ilmoniemi R, Knuutila J, Lounasmaa OV (1993) Magnetoencephalography: theory, instrumentation, and applications to noninvasive studies of the working human brain. Rev Mod Physics 65:413–497.

Hari R, Salmelin R (1997) Human cortical oscillations: a neuromagnetic view through the skull. Trends Neurosci 20:44–49.

Hari R, Karhu J, Hämäläinen M, Knnutila J, Salonen O, Sams M (1993) functional organization of the human first and second somatosensory cortices: a neuromagnetic study. Eur J Neurosci 5:724–734.
Hari R, Salmelin R, Tissari SO, Kajola M, Virsu V (1994) Visual stability during eyeblinks. Nature 367:121–122.
Heilman KM, Bowers D, Coslett HB, Whelan H, Watson RT (1985) Directional hypokinesia: prolonged reaction times for leftward movements in patients with right hemisphere lesions and neglect. Neurology 35:855–859.
Hyvärinen J (1981) Regional distribution of functions in parietal association area 7 of the monkey. Brian Res 206:287–303.
Hyvärinen J, Poranen A (1974) Function of parietal associative area 7 as revealed from cellular discharges in alert monkeys. Brain 97:673–692.
Jackson SR, Husain M (1997) Visual control of hand action. Trends Cognit Sci 1:310–317.
Jeannerod M, Arbib MA, Rizzolatti G, Sakata H (1995) Grasping objects: the cortical mechanisms of visuomotor transformation. Trends Neurosci 18:314–320.
Johnson PB, Ferraina S, Bianchi L, Caminiti R (1996) Cortical networks for visual reaching. Physiological and anatomical organization of frontal and parietal lobe arm regions. Cereb Cortex 6:101–119.
Jousmäki V, Hämäläinen M, Hari R (1996) Magnetic source imaging during a visually guided task. NeuroReport 7:2961–2964.
Keating EG (1991) Frontal eye field lesions impair predictive and visually-guided pursuit eye movements. Exp Brain Res 86:311–323.
Kleinschmit A, Merboldt KD, Requardt M (1994) Functional MRI of cooperative cortical activation patterns during eye movements. Soc Neurosci Abstr 20:1402.
Komatsu H, Wurtz RH (1988a) Relation of cortical areas MT and MST to pursuit eye movements. I. Localization and visual properties of neurons. J Neurophysiol 60:580–603.
Komatsu H, Wurtz RH (1988b) Relation of cortical areas MT and MST to pursuit eye movements. III. Interaction with full-field visual stimulation. J Neurophysiol 60:621–644.
Lacquaniti F, Perani D, Guigon E, Bettinardi V, Carrozzo M, Grassi F, Rossetti Y, Fazio F (1997) Visuomotor transformations for reaching to memorized targets: a PET study. NeuroImage 5:129–146.
Lekwuwa GU, Barnes GR (1996) Cerebral control of eye movements I. The relationship between cerebral lesion sites and smooth pursuit deficits. Brain 119:473–490.
Levänen S, Ahonen A, hari R, McEvoy L, Sams M (1996) Deviant auditory stimuli activate human left and right auditory cortex differently. Cereb Cortex 6:288–296.
Luna B, Thulborn KR, Strojwas MH, McCurtain BJ, Berman RA, Genovese R, Sweeney JA (1998) Dorsal cortical regions subserving visually guided saccades in human: an fMRI study. Cereb Cortex 8:40–47.
Lynch JC (1987) frontal eye field lesions in monkeys disrupt visual pursuit. Exp Brain Res 68:437–441.
Lynch JC, Mountcastle VB, Talbot WH, Yin TC (1977) Parietal lobe mechanisms for directed visual attention. J Neurophysiol 40:362–389.
Lynch JC, Graybiel AM, Lobeck LJ (1985) The differential projection of two cytoarchitectonic subregions of the inferior parietal lobule of macaque upon the deep layers of the superior colliculus. J Comp Neurol 235:241–254.
MacAvoy MG, Gottlieb JP, Bruce CJ (1991) Smooth-pursuit eye movement representation in the primate frontal eye field. Cereb Cortex 1:95–102.
Mattingley JB, Bradshwa JL, Phillips JG (1994) Impairments of movement execution in unilateral neglect: a kinematic analysis of directional bradykinesia. Neuropsychology 32:1111–1134.
Mattingley JB, Husain M, Rorden C, Kennard C, Driver J (1998) Motor role of human inferior parietal lobe revealed in unilateral neglect patients. Nature 392:179–182.
Maunsell JHR, Newsome WT (1987) Visual processing in monkey extrastriate cortex. Annu Rev Neurosci 10:363–401.
Maunsell JH, Van Essen DC (1987) Topographic organization of the middle temporal visual area in the macaque monkey: representational biases and the relationship to callosal connections and myeloarchitectonic boundaries. J Comp Neurol 266:535–555.
Mesulam MM (1981) A cortical network for directed attention and unilateral neglect. Ann Neurol 10:309–325.
Morrow MJ, Sharpe JA (1995) Deficits of smooth-pursuit eye movement after unilateral frontal lobe lesions. Ann Neurol 37:443–451.
Mosher JC, Lewis PS, Leahy RM (1992) Multiple dipole modeling and localization from spatio-temporal MEG data. IEEE Trans Biomed Eng 39:541–557.
Motter BC, Mountcastle VB (1981) The functional properties of the light-sensitive neurons of the posterior parietal cortex studied in waking monkeys: foveal sparing and opponent vector organization. J Neurosci 1:3–26.
Mountcastle VB, Lynch JC, Georgopoulos A, Sakata H, Acuna C (1975) Posterior parietal association cortex of the monkey: command functions for operations within extrapersonal space. J Neurophysiol 38:871–908.
Mountcastle VB, Andersen RA, Motter BC (1981) The influence of attentive fixation upon the excitability of the light-sensitive neurons of the posterior parietal cortex. J Neurosci 1:1218–1235.
Muri RM, Iba-Zizen MT, Derosier C, Cabanis EA, Pierrot-Deseillignuy C (1996) Location of the human posterior eye field with functional magnetic resonance imaging. J Neurol Neurosurg Psychiatry 60:445–448.
Neal JW, Pearson RC, Powell TP (1990) The ipsilateral cortico-cortical connections of area 7 with the frontal lobe in the monkey. Brain Res 509:31–40.
Nishitani N, Nagamine T, Fujiwara N, Yazawa S, Shibasaki H (1998) Cortical-hippocampal auditory processing identified by magnetoencephalography. J Cognit Neurosci 10:231–247.
Nobre AC, Sebestyen GN, Gitelman DR, Mesulam MM, Frackowiak RSJ, Frith CD (1997) Functional localization of the system for visuospatial attention using positron emission tomography. Brain 120:515–533.
Paus T (1996) Location and function of the human frontal eye field: a selective review. Neuropsychologia 34:475–483.
Perenin MT, Vighetto A (1988) Optic ataxia: a specific disruption in visuomotor mechanisms. I. Different aspects of the deficit in reaching for objects. Brain 111:643–674.
Petit L, Clark VP, Ingeholm J, Haxby JV (1997) Dissociation of saccade-related and pursuit-related activation in human frontal eye fields as revealed by fMRI. J Neurophysiol 77:3386–3390.
Pierrot-Deseillingny C (1994) Saccade and smooth-pursuit impairment after cerebral hemispheric lesions. Eur Neurol 34:121–134.
Pierrot-Deseilligny C, Rivaud S, Gaymard B, Muri R, Vermersch AI (1995) Cortical control of saccades. Ann Neurol 37:557–567.
Portin K, Salenius S, Salmelin R, Hari R (1998) Activation of the human occipital and parietal cortex by pattern and luminance stimuli: neuromagnetic measurements. Cereb Cortex 8:253–260.
Posner MI, Walker JA, Friedrich FJ, Rafal RD (1984) Effects of parietal injury on covert orienting of attention. J Neurosci 4:1863–1874.
Raij T, McEvoy L, Mäkelä JP, Hari R (1997) Human auditory cortex is activated by omissions of auditory stimuli. Brain Res 745:134–143.
Rivaud S, Muri RM, Gaymard B, Vererscn AI, Pierrot-Deseillingny C (1994) Eye movement disorders after frontal eye field lesions in humans. Exp Brain Res 102:110–120.
Rizzolatti G and Gallese V (1998) Mechanisms and theories of spatial neglect. Handb Neuropsychol 1:233–246.
Sakata H, Shibutani H, Kawano K (1983) Functional properties of visual tracking neurons in posterior parietal association cortex of the monkey. J Neurophysiol 49:1364–1380.
Sakata H, Taira M, Murata A, Mine S (1995) Neural mechanism of visual guidance of hand action in the parietal cortex of the monkey. Cereb Cortex 5:429–438.
Salenius S, Schnitzler A, Salmelin R, Jousmäki V, Hari R (1997) modulation of human cortical rolandic rhythms during natural sensorimotor tasks. NeuroImage 5:221–228.
Savaki HE, Raos VC, Dalezios Y (1997) Spatial cortical patterns of metabolic activity in monkeys performing a visually guided reaching task with one forelimb. Neuroscience 76:1007–1034.
Scherg M (1992) Functional imaging and localization of electromagnetic brain activity. Brain Topogr 5:103–111.
Scherg M, Von Cramon D (1986) Evoked dipole source potentials of the human auditory cortex. Electroencephalogr Clin Neurophysiol 65:344–360.
Snyder LH, Batista AP, Andersen RA (1997) Coding of intention in the posterior parietal cortex. Nature 386:167–170.
Stein JF (1992) The representation of egocentric space in the posterior parietal cortex. Behav Brain Sci 15:691–700.
Steinmetz MA, Constantinidis C (1995) Neurophysiological evidence for a role of posterior parietal cortex in redirecting visual attention. Cereb Cortex 5:448–456.

Sweeney JA, Luna B, Strojwas MH, Thulborn KR (1997) Mapping distinct cortical eye fields for saccadic and pursuit eye movement in humans using fMRI. Soc Neurosci Abstr 23:2222.

Talairach J, Tournoux P (1988) Co-planar stereotaxic atlas of the human brain 3-dimensional proportional system: an approach to cerebral imaging. Stuttgart: Georg Thieme Verlag.

Tanaka M, Fukushima K (1998) Neuronal responses related to smooth pursuit eye movements in the periarcuate cortical area of monkeys. J Neurophysiol 80:28–47.

Ungerleider LG, Desimone R (1986) Cortical connections of visual area MT in the macaque. J Comp Neurol 248:190–222.

Ungerleider LG, Mishkin M (1982) Two cortical visual systems. In: Analysis of visual behavior (Ingle DJ, Goodale MA, Mansfield RJW, eds), pp 549–586. Cambridge: MIT.

Uusitalo MA, Ilmoniemi RJ (1997) The signal-space projection (SSP) method for separating MEG or EEG into components. Med Biol Eng Comput 35:135–140.

Uutela KH, Hämäläinen MS, Somersalo E (1997) Spatial and temporal visualization of magnetoencephalographic data using minimum-current estimates. NeuroImage 5:S434.

Vallar G, Perani D (1986) The anatomy of unilateral neglect after right-hemisphere stroke lesions: a clinical/CT-scan correlation study in man. Neuropsychology 24:609–622.

Van Essen DC, Maunsell JH, Bixby JL (1981) The middle temporal visual area in the macaque: myeloarchitecture, connections, functional properties and topographic organization. J Comp Neurol 199:293–326.

Van Essen DC, Anderson CH, Felleman DJ (1992) Information-processing in the primate visual system: an integrated systems perceptive. Science 255:419–423.

Vanni S, Uusitalo MA, Kiesilä P, Hari R (1997) Visual motion activates V5 in dyslexics. NeuroReport 8:1939–1942.

Zeki SM (1974) Functional organization of a visual area in the posterior bank of the superior temporal sulcus of the rhesus monkey. J Physiol (Lond) 236:549–573.